CHAOS Theory and Applications in Applied Sciences and Engineering

e-ISSN: 2687-4539
RESEARCH ARTICLE
Vol.6 / No.2 / 2024 / pp.122-130
Special Issue (EDIESCA 2023)
https://doi.org/10.51537/chaos.1376501

Emergent Behaviors in Coupled Multi-scroll Oscillators in Network with Subnetworks

A. Ruiz-Silva[*,1], **B.B. Cassal-Quiroga**[α,2], **Eber J. Ávila-Martínez**[β,3] **and H.E. Gilardi-Velázquez**[§,4]

[*]Programa de Ingeniería en Sistemas Biomédicos. Universidad Estatal de Sonora, Unidad Hermosillo, Ley Federal del Trabajo, Col. Apolo, 83100, Hermosillo, Sonora, México, [α]Facultad de Ciencias, Universidad Autónoma de San Luis Potosí. Av. Chapultepec 1570, Priv. del Pedregal, 78295, San Luis Potosí, S. L. P., México, [β]Innovaciones Tecnológicas Mercado S.A. de C.V., Av. Sierra Leona 418, Lomas 2a Secc., 78210, San Luis Potosí, S.L.P., México, [§]Facultad de Ingeniería, Universidad Panamericana, Josemaría Escrivá de Balaguer 101,20296 Aguascalientes, Aguascalientes, Mexico.

ABSTRACT This paper presents the emergence of two collective behaviors in interconnected networks. Specifically, the nodes in these networks belong to a particular class of piece-wise linear systems. The global topology of the network is designed in the form of connected subnetworks, which do not necessarily share the same structure and coupling strength. In particular, it is considered that there are two levels of connection, the internal level is related to the connection between the nodes of each subnetwork; while the external level is related to connections between subnetworks. In this configuration, the internal level is considered to provide lower bounds on the coupling strength to ensure internal synchronization of subnetworks. The external level has a relevant value in the type of collective behavior that can be achieved, for which, we determine conditions in the coupling scheme, to achieve partial or complete cluster synchronization, preserving the internal synchronization of each cluster. The analysis of the emergence of stable collective behavior is presented by using Lyapunov functions of the different coupling. The theoretical results are validated by numerical simulations.

KEYWORDS
Network of subnetworks
Multi-scroll systems
Synchronization
PWL systems

INTRODUCTION

In recent years, there has been a growing interest in the study of networks containing subnetworks, spanning various scientific and technological fields. This is because studying interconnected networks plays a fundamental role in modeling systems composed of multiple interacting components (Huang *et al.* 2008; Mucha *et al.* 2010; Lu *et al.* 2014; Boccaletti *et al.* 2023). Usually, a network of subnetworks is considered to be composed of a large set of interconnected groups, where subnetworks, clusters, or communities can be identified, sharing a common topological or dynamic classification feature (Chen *et al.* 2014; Kenett *et al.* 2015). Furthermore, synchronization in complex dynamic networks has many applications in different fields as secure communications (Méndez-Ramírez *et al.* 2023; Zhou and Wang 2016).

Manuscript received: 6 October 2023,
Revised: 15 November 2023,
Accepted: 4 December 2023.

[1]adriana.ruiz@ues.mx (**Corresponding author**)
[2]bahia.cassal@uaslp.mx
[3]phd.eber.avila.martinez@gmail.com
[4]hgilardi@up.edu.mx

In this field, research approaches can be categorized into two main lines. The first line concentrates on the analysis of the structural or spectral properties of networks of subnetworks, with the primary objective of characterizing the "subnetwork structure" of a complex system. This involves the identification of groups of closely interconnected nodes that can address aspects such as transitivity, degree distribution, the presence of recurring patterns, as well as the spectral characteristics of their Laplacian matrices (De Domenico *et al.* 2013; Cozzo *et al.* 2016; Tang *et al.* 2023; Katakamsetty *et al.* 2023). The second research line focuses on the dynamic properties of networks of subnetworks, where each subnetwork is composed of nodes with similar or identical dynamic properties Kenett *et al.* (2015). In this context, the principal objective is to describe the development of collective motion within these subnetworks, which includes the observation of various patterns of synchronized behavior and other dynamic phenomena (Liu *et al.* 2023; Arellano-Delgado *et al.* 2023; Boccaletti *et al.* 2014, 2023; Lu *et al.* 2014).

Many recent studies have been dedicated to analyzing the emergence of collective behavior in subnetworks, often defining two types of collective behaviors: inner synchronization and outer synchronization. Usually, outer synchronization, also referred to as complete synchronization, happens when all nodes within a network of subnetworks synchronize their dynamics, demonstrating that same behavior or state. In outer synchronization, there is no distinction between nodes or subnetworks of nodes; instead, the entire network functions as a single coherent unit. This synchronization is typically observed in networks with strong couplings or interactions between nodes, where information and dynamics propagate swiftly throughout the network, resulting in a collective behavior where all nodes converge to the same state.

On the other hand, inner synchronization, also referred to as local synchronization or cluster synchronization, occurs when a subnetwork of nodes within a network achieve synchronization of their dynamics while maintaining distinct dynamics between the subnetwork or cluster (Ruiz-Silva and Barajas-Ramírez 2018; Ruiz-Silva 2021). In other words, nodes within each subnetwork synchronize with one another, while nodes in separate subnetworks exhibit distinct behaviors. Inner synchronization is often observed in networks with a modular or hierarchical structure, where nodes within the same module or hierarchy exhibit stronger synchronization with each other compared to nodes outside their respective module or hierarchy. It should be noted that most previous studies on cluster synchronization analyze the collective behavior for networks in which nodes are different systems where different emergent behaviors are mainly related to the nature of the nodes. However, there are few investigations focused on the synchronization problem for a set of dynamical systems that exhibit different collective behaviors in networks with identical nodes, where depending on the correlation between the states and the dynamical systems involved is the type of collective behavior that appears.

The simplest type of synchronization to identify is when states oscillate identically, and when they oscillate differently it is known as generalized synchronization. In particular, we consider piecewise linear systems, since represent a specific category of dynamic systems that display linear properties within discrete regions of their state space, delimited by potentially nonlinear boundaries. These systems have proven to be valuable tools for modeling a wide range of phenomena in various disciplines, from physics to biology and engineering. In this research, we focus on the analysis of networks whose nodes are piece-wise linear systems, adding a layer of complexity to the interconnected dynamics. The use of this type of system is attributed to its facilitation of stability analysis for network models. Furthermore, there exist prior results regarding the synchronization of these systems in regular network models (Ruiz-Silva *et al.* 2022b; Ávila-Martínez *et al.* 2022; Ruiz-Silva *et al.* 2022a).

In this work, our primary focus is on the exploration of the emergence of collective behaviors in interconnected subnetworks under changes in the nature of coupling scheme, which have been configured with two levels of interconnection. The internal level pertains to individual connections within each subnetwork, while the external level encompasses connections between different subnetworks. It is imperative to highlight that the external level serves a dual role, as it not only facilitates communication between subnetworks but also plays a crucial role in determining the collective behaviors observed in the entire network. Furthermore, in order to simplify the analysis, the nodes are regarded as a specific class of piece-wise linear systems capable to displays infinite scrolls along one-dimensional grid (Gilardi-Velázquez *et al.* 2017).

In particular, we consider a network of identical multiscroll systems where the coupling scheme is linear, bidirectional, and diffusive, for which the emergence of stable collective behavior is analyzed. For this purpose, we consider that systems are coupled by one, two, or three state variables. There is a theoretical analysis to determine the conditions under which synchronization arises using a common Lyapunov function for all the nodes in an unweighted network. The stabilization analysis, in the synchronization problem between clusters in a complex network, is interesting because the individual dynamics of each cluster can have a different qualitative behavior that depends on the initial conditions and its inner coupling, hence the steady state of the synchronous solution. It isn't easy to know it a priori due to sensitivity to initial conditions. Moreover, numerical simulations are used to illustrate the emergent behavior in the networks of multi-scrolls as partial and complete cluster synchronization.

The rest of the document is structured as follows: First, we introduce multi-scroll systems, the subnetwork model, and the construction of the subnetwork network model. Second, we analyze the synchronized behavior for a subnetwork and network of subnetworks using Lyapunov stability theory. Third, we present a case study, followed by numerical simulations that illustrate our result. Finally, we conclude with a discussion of our findings.

PRELIMINARIES

Multi-scroll System

In literature, various approaches have been proposed for generating attractors with multiple scrolls (Campos-Cantón *et al.* 2010; Echenausía-Monroy and Huerta-Cuéllar 2020). It is widely known that the generation of this type of attractor is influenced both by the stability properties of the generated equilibrium points and the choice of an appropriate switching function for implementation. In general terms, it is possible to evaluate the stability of the equilibrium points in these systems by applying the theory of Unstable Dissipative Systems (UDS). This theory is formulated within a three-dimensional manifold encompassing dissipative and conservative components. Consequently, the coexistence of these two components results in the emergence of attractors referred to as multi-scroll attractors (Campos-Cantón *et al.* 2012; Campos-Cantón 2016).

As a previous work (Gilardi-Velázquez *et al.* 2017), we consider that each node is a nonlinear dynamical system defined for a specific class of affine linear systems given by the round function which is defined as follows:

$$\begin{aligned} \dot{\psi}_i &= A\psi_i + B(\psi_i), \\ \begin{bmatrix} \dot{x}_i \\ \dot{y}_i \\ \dot{z}_i \end{bmatrix} &= \begin{bmatrix} y_i \\ z_i \\ -a_{31}x_i - a_{32}y_i - a_{33}z_i \end{bmatrix} + \begin{bmatrix} 0 \\ 0 \\ c * Round\left(\frac{x_i}{0.6}\right) \end{bmatrix}, \end{aligned} \quad (1)$$

where $\psi_i = [x_i, y_i, z_i]^T \in \mathbb{R}^3$ is the state vector of the i-th node, the constant matrix $A = \{a_{ij}\} \in \mathbb{R}^{3\times 3}$ is the linear operator of the system, and $B = [b_1, b_2, b_3]^T \in \mathbb{R}^3$ is the affine vector. It should be noted that the behavior of the system (1) is determined by the spectrum of matrix A, which can generate a wide variety of combinations and, therefore, various dynamic behaviors. In particular, (Gilardi-Velázquez *et al.* 2017) introduced a commutation law between different regions of the phase space, reflected in the affine vector B, which is controlled by the $Round(x)$ function. So that the system can show infinite scrolls along one dimension or infinite attractors for a specific bifurcation parameter, in this work we just consider the parameters for which the systems display infinite scrolls.

Under these conditions, an example of the system described in equation (1) is shown in Figure 1 for $a_{31} = 10.5$, $a_{32} = 7.0$, $a_{33} = 0.7$, and $c = 6.3$ with initial condition $\psi_0 = [3, -0.5, 0.5]^T$. In Figure 1(a) we show the projection of the multi-scroll system onto the planes (x_i, y_i), (x_i, z_i), and (y_i, z_i). Figure 1(b) corresponds to the temporal behavior of the states x_i, y_i, and z_i with arbitrary units (a.u.) time. Additionally, in Figure 2 we show the phase portrait of the resulting attractor.

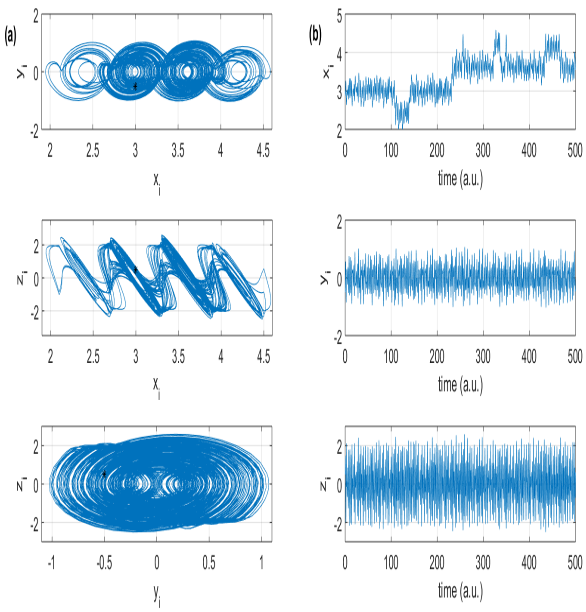

Figure 1 Projection of trajectories of the system (1) onto the the planes (x_i, y_i), (x_i, z_i) and (y_i, z_i), and time series with initial condition $\psi_0 = [3, -0.5, 0.5]^T$ marked by black asterisk.

Subnetworks model

Consider a regular dynamical subnetwork (RDS) formed by a set of r interconnected nodes, where each of the node is a multi-scroll system (1), and the interaction structure between them is modeled by a regular graph. Therefore, the individual dynamics of each node in the subnetwork of the RDS is given by:

$$\dot{\psi}_i^{[k]} = f(\psi_i^{[k]}) + g^{[k]} \sum_{j=1}^{r} \ell_{ij}^{[k]} \Gamma^{[k]} \psi_j^{[k]}, \text{ for } i = 1, 2, \cdots, r. \quad (2)$$

Here, the supra-index k indicates the label of each subnetwork, $\psi_i^{[k]} = [x_i^{[k]}, y_i^{[k]}, z_i^{[k]}]^T \in \mathbb{R}^3$ is the state vector of i-th node in k-th subnetwork; $f(\psi_i^{[k]}) = A\psi_i^{[k]} + B(\psi_i^{[k]})$ determines the dynamics of an isolated node, i.e., multi-scroll system. The constant $g^{[k]} > 0$ denotes the uniform coupling strength of the subnetwork; $\Gamma^{[k]} \in \mathbb{R}^{3\times 3}$ is a zero-one diagonal matrix describing the internal coupling between nodes in the k-th subnetwork. The Laplacian matrix gives its external coupling configuration for each subnetwork, $L^{[k]} = \{\ell_{ij}^{[k]}\} \in \mathbb{R}^{r\times r}$, which is considered to be a regularly connected graph. Furthermore, we assume that each subnetwork

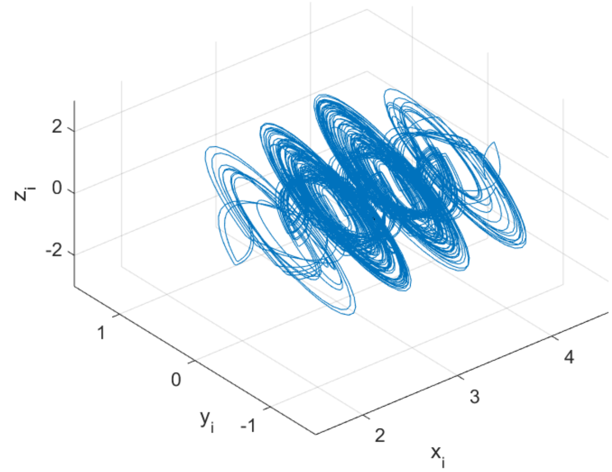

Figure 2 Multi-scroll attractor, in the phase space (x_i, y_i, z_i) with the initial condition $\psi_0 = [3, -0.5, 0.5]^T$.

is connected, *i.e.*, that there are no isolated nodes in the subnetwork. As a result, the Laplacian matrix, $L^{[k]}$, is a symmetric and irreducible matrix, with just one zero eigenvalue and all other eigenvalues strictly negative (Wang and Chen 2002).

Notice that in general, the set of admissible structures $L^{[k]}$ may include all possible patterns of connections. However, it is necessary to determine some restrictions when establishing the model for a network of subnetworks. Although they may be networks with different topologies, they must contain the same number of nodes.

Defining $\chi^k = [\psi_1^{[k]}, \psi_2^{[k]}, \cdots, \psi_r^{[k]}] \in \mathbb{R}^{3r}$ as the state variable of a single subnetwork. Then, (2) can be expressed as

$$\dot{\chi}^{[k]} = F^{[k]}(\chi^{[k]}, g^{[k]}, \Gamma^{[k]}, L^{[k]}). \quad (3)$$

In what follows we will use the following shorthand notation, $F^{[k]}(\chi^{[k]})$, for the dynamics of the k-th subnetwork, whose elements depend on the coupling matrix, the connection strength and the internal dynamics of the nodes.

Network of subnetworks

Now, consider that M subnetworks are interconnected in a network model. In this context, the dynamical equation of the full system is described as follows

$$\dot{\psi}_i^{[k]} = f(\psi_i^{[k]}) + g^{[k]} \sum_{j=1}^{r} \ell_{ij}^{[k]} \Gamma^{[k]} \psi_j^{[k]} + \sum_{l=1}^{M} d_{kl} H^{[l]} \psi_i^{[l]}, \quad (4)$$

for $i = 1, 2, \cdots, r$, and $k, l = 1, 2, \cdots, M$. Note that the first two terms on the right-hand side of (4) represent the individual dynamics of each subnetwork, whose elements were described in (2). While the third element to the right-hand side of (4) is related to the coupling among subnetworks.

Hence, $H^{[l]}$ is the inner connection matrix for nodes in different subnetworks, and the $D = \{d_{kl}\} \in \mathbb{R}^{M\times M}$ elements belong to the outer connection matrix for different subnetworks, which is constructed as follows: if a node in the k-th subnetwork is connected with its replica in the l-th subnetwork thus $d_{kl} \neq 0$ (with $k \neq l$), otherwise $d_{kl} = 0$, and $d_{kk} = -\sum_{l=1}^{M} d_{kl}$ for $k, l = 1, 2, \cdots, M$.

In vector form the eq. (4) can be written as:

$$\dot{\chi} = F(\chi) + (D \otimes H)\chi \tag{5}$$

where $\chi = [\chi^{[1]}, \chi^{[2]}, \cdots, \chi^{[M]}]^T \in \mathbb{R}^{3rM}$, is the state equations of the networks of subnetworks, with $\chi^{[k]} \in \mathbb{R}^{3r}$; $D \in \mathbb{R}^{M\times M}$ is the outer connection matrix described in the previous paragraph, while $H = Diag(H^{[1]}, H^{[2]}, \cdots, H^{[M]}) \in \mathbb{R}^{3r\times 3r}$, and $\otimes$ denotes the Kronecker product. It is worth noting that the network model describes all kinds of topologies, where they can consider connection patterns with uniform weights or non-uniform connections.

An example of our proposed structures is shown in Figure 3. In this case, both networks are composed of six subnetworks made up of $r = 4$ nodes, each of the subnetworks is represented by a color, and black lines represent the connections between the subnetworks. In Figure 3(a) all subnetworks have a star structure with a bidirectional coupling. Additionally, the connection between subnetworks is through a bidirectional ring structure. In Figure 3(b) the subnetworks have different topologies, and the connection between subnetworks is shown with some directed links.

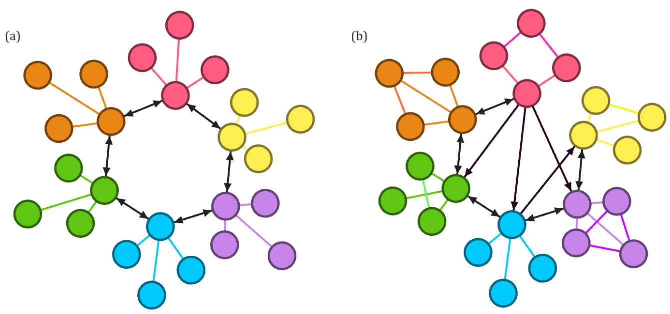

Figure 3 Two schematic illustrations of a network consisting of six subnetworks. Each subnetwork is represented by a color, and black lines represent the connections between subnetworks.

For complex dynamical networks, one of the most investigated collective behavior is synchronization, which occurs when the dynamics of its nodes are correlated over time (Chen *et al.* 2014; Pecora and Carroll 1998; Arenas *et al.* 2008). There are several definitions of synchronization among nodes in a network (Arenas *et al.* 2008). Even the definitions can be extended when considering the synchronization problem in a group of interconnected subnetworks.

In this paper, we will mainly focus on complete synchronization when discussing the subnetwork model. According to (Chen *et al.* 2014; Ruiz-Silva *et al.* 2021), a subnetwork of uniform, linearly, and diffusively coupled identical dynamical systems with a state equations description given by (2) is said to achieve (asymptotically) synchronization, if all the solutions converge to the same solution $s^{[k]}$ as t tends to infinity. For any initial condition in the neighborhood of the synchronization solution, one has that

$$\lim_{t\to\infty} \|\psi_i^{[k]} - s^{[k]}\| = 0, \text{ for } i = 1, 2, \cdots, r. \tag{6}$$

where $s^{[k]} \in \mathbb{R}^3$ satisfies the dynamics of an isolated multi-scroll attractor $\dot{s}^{[k]} = A(s^{[k]}) + B(s^{[k]})$.

To demonstrate that each subnetwork achieves the synchronization there are different methodologies. Following the proposal in (Ruiz-Silva *et al.* 2021) where they define the error as $e_i = \psi_i^{[k]} - s^{[k]}$ for each $i = 1, 2, \cdots, r$, and the error dynamics are linearized around the synchronization solution and diagonalized in terms of the eigenvalues of the Laplacian matrix for a subnetworks, resulting in the λ_2 criterion for the stability of the synchronized solutions. Therefore, the following Theorem has been reconstructed to establish *complete synchronization* on subnetwork:

Theorem 1 *(Ruiz-Silva et al. 2021) The RDS (2) achieves the complete synchronization (5). If the internal coupling matrix $\Gamma^{[k]} \in \Gamma_{cs}$ with*

$$\Gamma_{cs} = \{Diag(1,1,1),\ Diag(1,0,1),\ Diag(1,1,0),\ Diag(1,0,0)\}, \tag{7}$$

and the coupling strength, $g^{[k]} \in \mathbb{R}_+$ satisfies the condition:

$$g^{[k]} \geq \frac{|d^*|}{|\lambda_2^{[k]}|} \tag{8}$$

where d^* is a non-positive constant, and $\lambda_2^{[k]}$ is the largest nonzero eigenvalues of $L^{[k]} \in \mathbb{R}^{r\times r}$.

The above theorem is a useful result to simplify the analysis of the collective behaviors that can arise in a network of subnetworks. Therefore, when each subnetwork has completely synchronized the solution to (2) has r identical components $s^{[k]} \in \mathbb{R}^3$, which we write as $S^{[k]} = [s^{[k]}, s^{[k]}, \cdots, s^{[k]}]^T \in \mathbb{R}^{3r}$.

In this paper, our aim is to find sufficient conditions for the interconnected subnetwork to achieve different collective behavior. Since that we assume that each subnetwork achieves complete synchronization then the global analysis of collective behavior can be transformed into the synchronization problem for a weighted network. In this context, the complete and cluster synchronization between subnetworks is defined as follows:

Definition 1 *The network of subnetworks (4) is said to achieve identical synchronization, if*

$$\lim_{t\to\infty} \|S^{[k]} - S^{[l]}\| = 0, \text{ for } k, l = 1, 2, \cdots, M \tag{9}$$

where the symbols $\|\cdot\|$ is the Euclidean norm of a vector, and $S^{[k]}$ and $S^{[l]}$ are the synchronous solutions of the k-th and l-th subnetworks, respectively.

Definition 2 *The network of subnetworks (4) is said to achieve cluster synchronization, if nodes in the same subnetwork achieves the complete synchronization, in the sense of equation (6), and the differences among the synchronization solutions of different subnetworks do not converge to zero, i.e.,*

$$\lim_{t\to\infty} \|S^{[k]} - S^{[l]}\| = \epsilon, \text{ for } k, l = 1, 2, \cdots, M \tag{10}$$

where $\epsilon \in \mathbb{R}+$, and $S^{[k]}$ and $S^{[l]}$ are the synchronous solutions of the k-th and l-th subnetworks, respectively.

Synchronization stability analysis

To begin our analysis of the emergence of synchronized behavior in the network of subnetworks, we have the following assumptions:

A1. The interconnected subnetworks contain the same number of nodes.

A2. For simplicity, the inner connected matrices $H^{[l]}$ are the same throughout the network of the subnetworks model to be studied.

A3. From each weighted outer connected matrix D we obtain the unweighted matrix $\mathcal{B}$ whose elements are

$$b_{kl} = \begin{cases} 1 & d_{kl} \neq 0 \\ 0 & d_{kl} = 0 \end{cases}, \text{ for } k, l = 1, 2, \cdots, M \text{ and } k \neq l. \quad (11)$$

and $b_{kk} = -\sum_{k=1, k\neq l}^{M} b_{kl}$. Also, these matrices satisfy the following condition

$$\lambda_2(D) \leq \tilde{d}\lambda_2(\mathcal{B}). \quad (12)$$

Similar to the case of a simple network, we need to find sufficient conditions to achieve complete synchronization or cluster synchronization. Firstly, we assume that there exists a global synchronization solution $S \in \mathbb{R}^{3rM}$, to which all subnetworks are synchronized so that analysis can be carried out. Here, the synchronization solution, S, may be an equilibrium point of the subnetwork, the average dynamics of all subnetworks, some periodic orbit, or a chaotic solution. Therefore, we define the error as $E_k = S^{[k]} - S$ for $k = 1, 2, \cdots, M$, and its variational equation as follow

$$\dot{E}_k = F(E_k + S) - F(S) + \sum_{j=1}^{M} d_{kl} H E_l \quad (13)$$

The stability of the solution $S^{[k]}$ for the subnetwork interconnected in a weighted network can be established following a similar procedure as in (Ruiz-Silva *et al.* 2021; Ruiz-Silva and Barajas-Ramírez 2018). That is, by establishing stability conditions for an unweighted network, and the difference between the weighted and unweighted outer Laplacian matrices, we obtain sufficient conditions to guarantee synchronization. The result is stated in the following result:

Theorem 2 *Consider a dynamical network of M identical subnetworks* (4)*, which satisfy conditions the Asssumptions* ***A1.*** *and* ***A2.****. If the elements of the outer connection matrix D satisfies*

$$d_{kl} \geq \frac{|d^*|}{|\mu_2|}, \quad (14)$$

where d^* is a non-negative constant and μ_2 is the second largest eigenvalue of the unweighted outer connection matrix (Assumption ***A3.****), then $E_k = 0$ for all $k = 1, 2, \cdots, M$. Consequently, the network of subnetworks achieves synchronization.*

Proof: To prove the stability of the systems (13) a Lyapunov function is chosen as follows: $V = \frac{1}{2}\sum_{k=1}^{M} E_k^\top E_k > 0$. The time derivate of V along the trajectories of (13) gives:

$$\dot{V} = \sum_{k=1}^{M} E_k^T \Big(F(E_k + S) - F(S) + \sum_{l=1}^{M} d_{kl} H E_l \Big) \quad (15)$$

Assuming that each subnetwork is a connected graph, which achieves internal synchronization, it is considered that the dynamics of each subnetwork are bounded by

$$\|F(E_k + S) - F(S)\| \leq d\|E_k\|. \quad (16)$$

where d is a non-negative real number, which is related to a limit for the dynamics of each subnetwork in isolation. Due to the eigenvalues of the external coupling matrix D can be sorted in ascending order, this implies that $\bar{\mu}_k \leq \bar{\mu}_2$, and holds

$$\begin{aligned} \dot{V} &\leq \sum_{k=1}^{M} \Big(dE_k^\top E_k + \sum_{l=1}^{M} E_k^\top (\bar{\mu}_2 H) E_l \Big) \\ &\leq \sum_{k=1}^{M} \Big(d\|E_k\|^2 - \bar{\mu}_2 h \sum_{l=1}^{M} \|E_k\| \|E_l\| \Big) \end{aligned} \quad (17)$$

where $h > 0$ is the largest eigenvalue of the inner connection matrix. The right-hand side of (17) is quadratic in $p = (\|E_1\|, \|E_2\|, \cdots, \|E_M\|)^\top$, which can be written as $\dot{V} = -p^\top \Phi p$, whose elements are defined by

$$\phi_{kl} = \begin{cases} d - \bar{\mu}_2 h & l = k \\ -\bar{\mu}_2 h & l \neq k \end{cases} \quad (18)$$

If one choose $d \leq \bar{\mu}_2 h$, then $\Phi \geq 0$. If follows that $\dot{V} \leq 0$. Now to guarantee that the derivative of the Lyapunov function is strictly negative, we use the properties of the weighted and unweighted outer connection matrices.

Since the outer connection matrix satisfies the assumption **A3**. It follows that there exists a positive constant $\bar{d}$ such that the matrices satisfy $\bar{d}\mathcal{B} \geq D$. It is known that both matrices are negative semidefinite, which implies that their second largest non-zero eigenvalues are: $\mu_2 < 0$ for the weighted connection matrix and $\bar{\mu}_2 < 0$ for the unweighted connection matrix. Therefore,

$$\mu_2 \leq \bar{d}\bar{\mu}_2 \quad (19)$$

Additionally, individually the elements of the weighted matrix satisfy

$$d_{kl} > \bar{d} \; for \; k \neq l \;\; k, l = 1, 2, \cdots, M \quad (20)$$

Now, defining a constant $d^* = d/h$ such that $d^* > d$, and using the (19)-(20), the condition (14) is obtained.

□

It is important to emphasize that the previous problem provides us with sufficient conditions for the error to be asymptotically stable. However, to achieve identical synchronization of the network of networks, the inner connection matrices of each subnetwork $H^{[l]}$ play a very important role because these matrices must be a combination of the matrices of the equation (7). So that the error in all states of the network is exactly zero. On the other hand, if the matrix H is made up of any linear combination that does not connect the first state of each node, then identical synchronization cannot be achieved, for these cases, the type of synchronization achieved is by cluster. To compactly express the previous discussion, the following two corollaries are extended from the theorem.

Corollary 1 Ruiz-Silva et al. (2022b) *The network of subnetworks* (4) *achieves the identical synchronization* (9)*. If the elements of the outer connection matrix* (14)*, and all inner connection matrix $H^{[l]}$ belongs to*

$$\{Diag(1,1,1),\; Diag(1,0,1),\; Diag(1,1,0),\; Diag(1,0,0)\} \quad (21)$$

for all $k = 1, 2, \cdots, M$.

Corollary 2 Ruiz-Silva et al. (2022b) *The dynamical network* (4) *achieves the cluster synchronization* (10)*. If the elements of the outer connection matrix* (14)*, and some of the inner connection matrix $H^{[l]}$ belongs to*

$$\{Diag(0,1,0), Diag(0,0,1),\; Diag(0,1,1)\}, \quad (22)$$

for all $k = 1, 2, \cdots, M$.

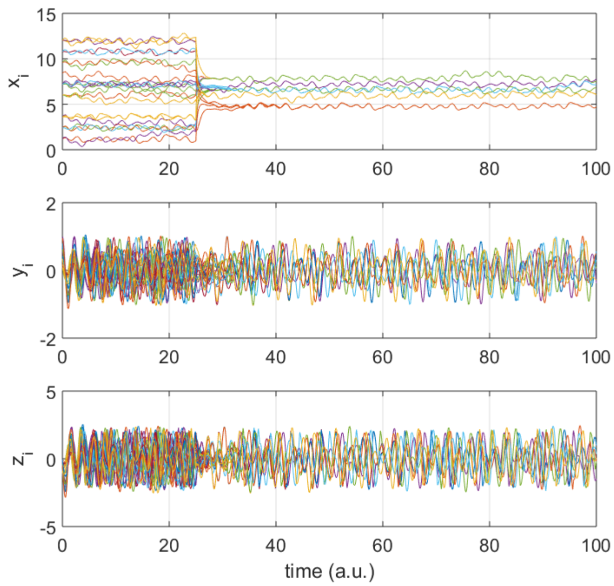

Figure 4 Numerical simulation of six decoupled subnetworks with an internal coupling matrix $\Gamma^{[k]} = Diag(1,0,1)$ for $k = 1,2,\cdots,M$, and the coupling strengths are: $g^{[1]} = 1$, $g^{[2]} = 2$, $g^{[3]} = 1.5$, $g^{[4]} = 3$, $g^{[5]} = 2.3$, $g^{[6]} = 4$

NUMERICAL SIMULATIONS

We consider a network of $M = 6$ subnetworks each made up of 4 identical multi-scroll systems (1). Thus, we describe the RDS model by equation (2) whose topology to use is a star graph (see Figure 3(a)).

First, it is necessary to ensure that identical synchronization is achieved within each RDS. In this example, let the internal coupling matrix $\Gamma = Diag(1,0,1)$ for each RDS. Consequently, condition (7) of Theorem 1 is satisfied, so it is necessary to obtain the appropriate critical value, d^*, associated with the internal matrix (see table 1). Finally, we calculate the minimum coupling strength to achieve synchronization, that is,

$$g^{[k]} > \frac{|d^*|}{|\lambda_2^k|} = \frac{0.9}{1}, \quad \text{for } k = 1,2,\cdots,M. \tag{23}$$

For this example, it is possible to choose the coupling strengths $g^{[1]} = 1$, $g^{[2]} = 2$, $g^{[3]} = 1.5$, $g^{[4]} = 3$, $g^{[5]} = 2.3$, $g^{[6]} = 4$, with which the conditions (7) of Theorem 1 are satisfied.

To illustrate the above in more detail, Figure 4 shows the time series of the subnetworks, with randomly chosen initial conditions. In numerical simulations, it is assumed that for t < 25 (a.u.) the nodes are decoupled so that each solution evolves its own attractor. While for t $\geq$ 25 (a.u.) the multi-scroll are connected in a subnetwork structure with a respective coupling strength. Moreover, for each subnetwork. In the first state of the nodes it is easy to observe how the trajectories collapse into six solutions, each one belonging to the synchronous state of each subnetwork.

Complete synchronization

Now, to illustrate complete synchronization in a network of subnetworks, we consider that the inner connection matrices described in Equation (21), particularly for $H^{[l]} = Diag(1,0,0) \in \mathbb{R}^{3\times 3}$ for $l = 1, 2, \cdots, M$, satisfying Corollary 1. Moreover, using the Table 1 we obtain the critical value for the entries of the outer Laplacian matrix, whose elements must satisfy the Theorem 2 equation (14), i.e.,

$$d_{kl} > \frac{|d^*|}{|\mu_2|} = \frac{3}{1}, \quad for \;\; k \neq l \tag{24}$$

and $k,l = 1,2,\cdots,M$. Consequently, we select the external connection matrix as:

$$\begin{pmatrix} -6.6 & 3.1 & 0 & 0 & 0 & 3.5 \\ 3.1 & -7.1 & 4 & 0 & 0 & 0 \\ 0 & 4 & -7.1 & 3.1 & 0 & 0 \\ 0 & 0 & 3.1 & -11.1 & 8 & 0 \\ 0 & 0 & 0 & 8 & -11 & 3 \\ 3.5 & 0 & 0 & 0 & 3 & -6.5 \end{pmatrix}. \tag{25}$$

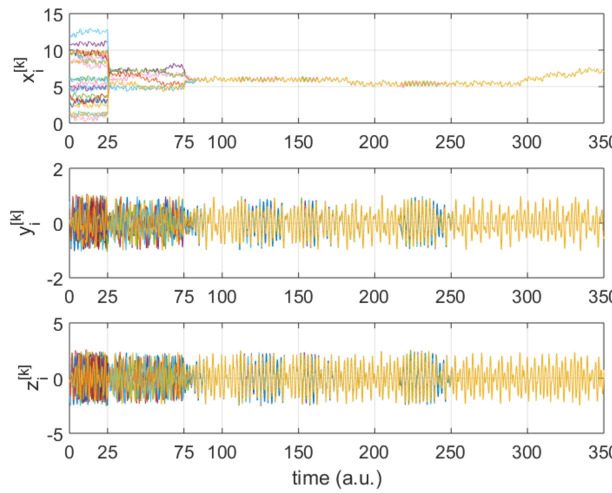

Figure 5 Numerical simulations of a network of six subnetworks interconnected in a ring structure, where the inner connection matrices are: $H^{[l]} = Diag(1,0,0)$ for $l = 1,2,\cdots,6$.

The results of the numerical simulation are presented in Figures 5. First, for times less than 25, the 24 multi-scrolls of the global network are decoupled. At time 25, each of the subnetworks is individually connected with the aforementioned coupling strength, $g^{[k]}$. Furthermore, in the numerical simulation corresponding to the first state of the systems it is possible to observe how the 24 individual solutions collapse into six different solutions, that is, the synchronization solution of each subnetwork.

Finally, starting at time 75, the subnetworks are connected to each other, generating the entire network of the subnetworks model. Here, it can be observed how the trajectories of all subnetworks collapse in the three states, i.e., the nodes achieve complete synchronization. It is important to note that the synchronization solution location is related to the mean of each state for both cases: the subnetwork and the entire network (Ruiz-Silva *et al.* 2022b).

In Figure 6, we show the error synchronization between nodes that belong to different subnetworks. Since the subnetworks archive the complete synchronization, we can observe that the error converges to zero in the three states.

Table 1 Bounded of d^* for each internal coupling matrix

Γ	d^*	Γ	d^*
$Diag(1,1,1)$	0.6	$Diag(0,1,0)$	3.4
$Diag(1,0,1)$	0.9	$Diag(0,0,1)$	1.8
$Diag(1,1,0)$	0.32	$Diag(0,1,1)$	0.6
$Diag(1,0,0)$	3		

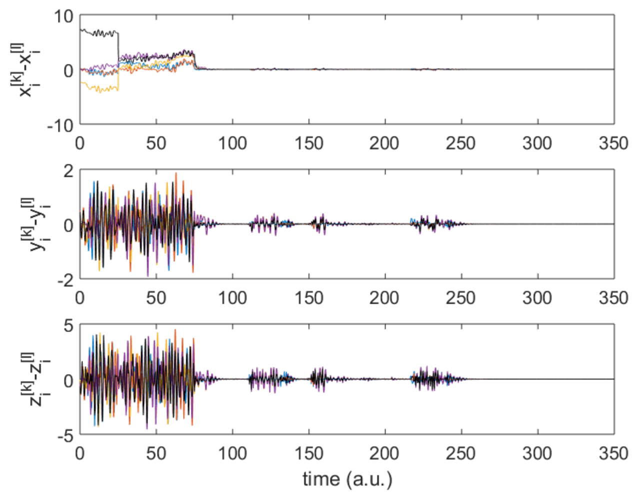

Figure 6 Evolution of the error synchronization between nodes of different subnetworks

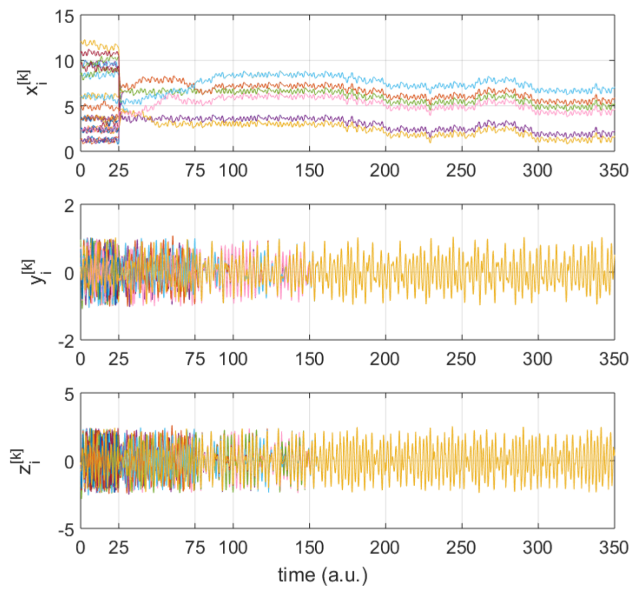

Figure 7 Numerical simulations of a network of six subnetworks interconnected in a ring structure, where the inner connection matrices are: $H^{[l]} = Diag(0,1,1)$ for $l = 1, 2, \cdots, 6$.

Cluster synchronization

For the cluster synchronization model, the same structure of the network of subnetworks is considered (see Figure 3 (a)), only that the association matrices between subnetworks described in eq. (22) particularly for $H^l = Diag(0,1,1)$ for $l = 1, 2, \cdots, 6$, satisfying Corollary 2.

Analogously to what is calculated in complete synchronization, the connection strength between the subnetworks can be calculated with Theorem 2, specifically with Equation (14). Under the proposed connection scheme, the critical value of d^* is 0.6 (see Table 1). Therefore, the elements of the external coupling matrix must satisfy

$$d_{kl} > \frac{|d^*|}{|\mu_2|} = \frac{0.6}{1}, \quad for \ \ k \neq l, \tag{26}$$

and $l = 1, 2, \cdots, 6$. It is easy to verify that the elements of the matrix (25) satisfy the previous condition. Therefore, it is the matrix that we will use for this scheme. The results of the numerical simulation are presented in Figure 7 where the dynamics of the six subnetworks are shown. First, for times less than 25, the 24 multi-scrolls of the global network are decoupled. At time 25, each of the subnetworks is individually connected with the aforementioned coupling strength, $g^{[k]}$.

For simulation times less than 75 a.u., it is possible to observe the six synchronous solutions of each uncoupled subnetwork. Subsequently, starting at time 75 the subnetworks are connected to each other, it can be observed how the trajectories of all subnetworks collapse in two states, but they are kept separate in the first state, *i.e.* the complete synchronization in each subnetwork is preserved but the subnetworks reach partial synchronization between them. This can also be observed in Figure 8, note that the error between the nodes that connect the subnetworks are shown, where the error in the first state remains constant, and for the state two and three the error converges to zero.

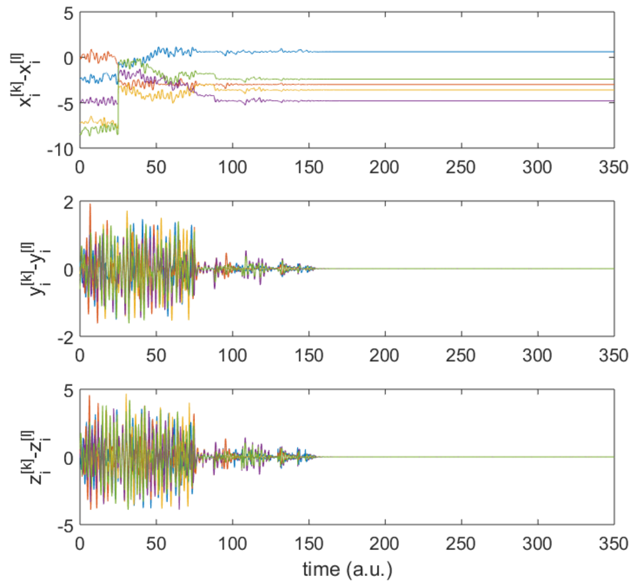

Figure 8 Evolution of the error synchronization between nodes of different subnetworks.

CONCLUSION

Our work focused on studying the synchronization of a set of coupled subnetworks and the emergence of collective behaviors in interconnected subnetworks when the coupling scheme changes. We considered subnetworks coupled by one, two, or three state variables and found two emerging behaviors in the synchronization state: complete and partial cluster synchronization. The results were validated using complex network theory and Lyapunov stability analysis and numerical simulations. In the first instance, we analyze a subnetwork of mutually coupled systems with uniform coupling strength, which must achieve complete synchronization to simplify the synchronization problem of a network of subnetworks. Furthermore, it is considered that the subnetworks have the same number of nodes and the same structure, so as not to have to perform an analysis to determine the node or nodes that should be interconnected between subnetworks. As a second instance, our analysis focused on the synchronization problem for subnetworks, where the outer connection matrix is crucial in determining the collective behavior of the network of subnetworks. In summary, this study delves into the emergence and characterization of collective behaviors in interconnected subnetworks. We strongly believe that the methodology discussed here can be applied to a subnetwork whose node dynamics are given by a broad class of PWL systems.

As future studies, it would be interesting to verify that the synchronization results can be extended to subnetworks with different structures or sizes, or even change the linear coupling between subnetworks.

Acknowledgments

Cassal-Quiroga B. B. (CVU:424203) acknowledges CONAHCYT financial support through the program "Estancias Posdoctorales por México 2022(1)".

Availability of data and material

Not applicable.

Conflicts of interest

The authors declare that there is no conflict of interest regarding the publication of this paper.

Ethical standard

The authors have no relevant financial or non-financial interests to disclose.

LITERATURE CITED

Arellano-Delgado, A., R. M. López-Gutiérrez, M. Á. Murillo-Escobar, and C. Posadas-Castillo, 2023 Master–slave outer synchronization in different inner–outer coupling network topologies. Entropy **25**: 707.

Arenas, A., A. Díaz-Guilera, J. Kurths, Y. Moreno, and C. Zhou, 2008 Synchronization in complex networks. Physics reports **469**: 93–153.

Ávila-Martínez, E. J., J. L. Echenausía-Monroy, and A. Ruíz-Sílva, 2022 Multi-scroll systems synchronization on strongly connected digraphs. Chaos Theory and Applications **4**: 205–211.

Boccaletti, S., G. Bianconi, R. Criado, C. I. Del Genio, J. Gómez-Gardenes, *et al.*, 2014 The structure and dynamics of multilayer networks. Physics reports **544**: 1–122.

Boccaletti, S., P. De Lellis, C. del Genio, K. Alfaro-Bittner, R. Criado, *et al.*, 2023 The structure and dynamics of networks with higher order interactions. Physics Reports **1018**: 1–64.

Campos-Cantón, E., 2016 Chaotic attractors based on unstable dissipative systems via third-order differential equation. International Journal of Modern Physics C **27**: 1650008.

Campos-Cantón, E., J. G. Barajas-Ramirez, G. Solis-Perales, and R. Femat, 2010 Multiscroll attractors by switching systems. Chaos: An Interdisciplinary Journal of Nonlinear Science **20**.

Campos-Cantón, E., R. Femat, and G. Chen, 2012 Attractors generated from switching unstable dissipative systems. Chaos: An Interdisciplinary Journal of Nonlinear Science **22**.

Chen, G., X. Wang, and X. Li, 2014 Fundamentals of complex networks : models, structures, and dynamics .

Cozzo, E., G. F. de Arruda, F. A. Rodrigues, and Y. Moreno, 2016 Multilayer networks: metrics and spectral properties. Interconnected networks pp. 17–35.

De Domenico, M., A. Solé-Ribalta, E. Cozzo, M. Kivelä, Y. Moreno, *et al.*, 2013 Mathematical formulation of multilayer networks. Physical Review X **3**: 041022.

Echenausía-Monroy, J. and G. Huerta-Cuéllar, 2020 A novel approach to generate attractors with a high number of scrolls. Nonlinear Analysis: Hybrid Systems **35**: 100822.

Gilardi-Velázquez, H. E., L. Ontañón-García, D. G. Hurtado-Rodriguez, and E. Campos-Cantón, 2017 Multistability in piecewise linear systems versus eigenspectra variation and round function. International Journal of Bifurcation and Chaos **27**: 1730031.

Huang, L., Y.-C. Lai, and R. A. Gatenby, 2008 Alternating synchronizability of complex clustered networks with regular local structure. Physical Review E **77**: 016103.

Katakamsetty, V. R., D. Rajani, and P. Srikanth, 2023 A study on community detection in multilayer networks. Journal of High Speed Networks pp. 1–13.

Kenett, D. Y., M. Perc, and S. Boccaletti, 2015 Networks of networks–an introduction. Chaos, Solitons & Fractals **80**: 1–6.

Liu, S., B. Xu, Q. Wang, and X. Tan, 2023 Synchronizability of multilayer star-ring networks with variable coupling strength. Electronic Research Archive **31**: 6236–6259.

Lu, R., W. Yu, J. Lü, and A. Xue, 2014 Synchronization on complex networks of networks. IEEE transactions on neural networks and learning systems **25**: 2110–2118.

Méndez-Ramírez, R., A. Arellano-Delgado, and M. Á. Murillo-Escobar, 2023 Network synchronization of macm circuits and its application to secure communications. Entropy **25**: 688.

Mucha, P. J., T. Richardson, K. Macon, M. A. Porter, and J.-P. Onnela, 2010 Community structure in time-dependent, multiscale, and multiplex networks. science **328**: 876–878.

Pecora, L. M. and T. L. Carroll, 1998 Master stability functions for synchronized coupled systems. Physical review letters **80**: 2109.

Ruiz-Silva, A., 2021 Synchronization patterns on networks of pancreatic β-cell models. Physica D: Nonlinear Phenomena **416**: 132783.

Ruiz-Silva, A. and J. G. Barajas-Ramírez, 2018 Cluster synchronization in networks of structured communities. Chaos, Solitons & Fractals **113**: 169–177.

Ruiz-Silva, A., B. Cassal-Quiroga, and H. Gilardi-Velázquez, 2022a Anti-synchronization in a pair of coupled multistable systems. In *Complex Systems and Their Applications: Second International Conference (EDIESCA 2021)*, pp. 23–37, Springer.

Ruiz-Silva, A., B. Cassal-Quiroga, G. Huerta-Cuellar, and H. Gilardi-Velázquez, 2022b On the behavior of bidirectionally coupled multistable systems. The European Physical Journal Special Topics **231**: 369–379.

Ruiz-Silva, A., H. Gilardi-Velázquez, and E. Campos, 2021 Emergence of synchronous behavior in a network with chaotic multistable systems. Chaos, Solitons & Fractals **151**: 111263.

Tang, F., X. Zhao, and C. Li, 2023 Community detection in multilayer networks based on matrix factorization and spectral embedding method. Mathematics **11**: 1573.

Wang, X. F. and G. Chen, 2002 Synchronization in small-world dynamical networks. International Journal of Bifurcation and chaos **12**: 187–192.

Zhou, L. and C. Wang, 2016 Hybrid combinatorial synchronization on multiple sub-networks of complex network with unknown boundaries of uncertainties. Optik **127**: 11037–11048.

How to cite this article: Ruiz-Silva, A., Cassal-Quiroga, B.B., Ávila-Martínez, E.J., and Gilardi-Velázquez, H.E. Emergent Behaviors in Coupled Multi-scroll Oscillators in Network with Subnetworks. *Chaos Theory and Applications*, 6(2), 122-130, 2024.